Investigation of Nickel Phthalocyanine Thin Films for Solar Cell Applications

Eman M. Nasir, Mohammed T. Hussein, Addnan H. Al-Aarajiy

Department of Physics, College of Science, University of Baghdad, Baghdad, Iraq
Email: eman.itabi@gmail.com

Abstract

Ni-Phthalocyanine thin films were thermally evaporated with different substrate temperatures (300 - 450) K on (silicon wafer, glass) substrates. The chemical bonds of NiPc powder were investigated by FTIR spectrum, which introduce good information for NiPc bonds and their locations. The optical properties have been studied by UV-Visible, and Photoluminescence (PL) Spectra. The NiPc thin films have direct gap for all samples. The values of energy gap which is calculated by PL spectra are lower than those calculated by Tauc equation. It is found there are three activation energies, the mobility and concentration of carriers have been measured and, the NiPc films are p-type. P-NiPc/n-Si HJ solar cell was fabricated at substrates temperatures (300, 400) K. From I-V and C-V characteristic, abrupt junction has been found, photovoltaic characteristics have been observed with Voc of (0.335 - 0.415) V, and Isc of (2.77 - 4.26) μA, and the efficiency of (3.08 - 5.03)% at room temperature and substrate temperature (300, 400 K) and under illumination of 55 mW/cm^2 using Halogen lamp. Ideality factors of the junction increase from (0.61 - 0.73) and barrier height increases from 2.53 eV to 3.69 eV while shunt resistance decreases from 3.76 KΩ to 2.59 KΩ and series resistance decreases slightly from 0.24 KΩ to 0.23 KΩ. The fill factor decreases from 0.46 to 0.4 with the increase of substrate temperature.

Keywords

Nickel Phthalocyanine, Optical Property, Electrical Property, Photoluminescence, Solar, Cell

1. Introduction

Phthalocyanines are regarded as optical materials. The optical film properties analysis explains the identity of materials and the correlation between theoretical and experimental work [1]. Inorganic materials have attracted attention as novel

material due to their chemical stability, low heat conduction, and diversity of optical properties and wide application in optoelectronic devices [2] [3]. Phthalocyanine can be considered as active materials in different light processes [4]. By discovering phthalocyanine since 1907, many studies on the optical properties have been achieved [5] [6]. There is a great interest in studying the electronic structure of phthalocyanine because of its high absorption in the visible region [7] [8] [9] [10]. Phthalocyanine happens in three phases (α, β, γ); the molecules are distributed in a parallel to each other leading to forming vertical structure in α phase and β phase, and in α-phase, phthalocyanine contains crystalline grain with 10 nm of diameter, whereas β phase contains bigger crystalline grain and fiber optical structure and this phase is formed at higher temperature. Many methods have been used to prepare metal phthalocyanine films [11]. Most of the metals have been able to coordinate with the phthalocyanine. Metal phthalocyanine (MPc) has great attractive as catalysts for organic chemical sensor and solar cell application due to simple prepared technique, low cost and stability for chemical and thermal properties [8]. NiPCs have α-phase and monoclinic structure, with $\beta = 123.46°$ and lattice constant a = 1.513 nm, b = 0.462 nm, c = 2.03 nm [9]. Organic semiconductor NiPCs contain single bond and double bonds [10]. The microscopic characteristic of the material can be known by studying optical measurements of film and this gives important information to build electronic devices [12]. The objectives of this work are the synthesis of thermally evaporated NiPc film using thermal evaporation technique, to study some of the properties at various T_s, also to prepare solar cell from n-Nickel Phthalocyanine: p-Silicon HJ and to study their properties.

2. Experimental

NiPc thin films at different substrate (300 - 450 K) were prepared by thermal evaporation (Edwards 306 systems) on (glass, n-Silicon) by using NiPc powder obtained from Aldrich chemical company. NiPc thin films were grown with a thicknesses of (50, 110, 265 and 350) nm on glass and on Si wafer substrates at room temperature. Also NiPCs film was grown in T_s (300, 325, 350, 400, 450) K with a thickness 265 nm, under vacuum pressure 10^{-5} torr.

Fourier-transformed Infra-red spectra for NiPc as a powder were measured by (Shimadzu FTIR spectrometer). The optical property of NiPc film was determined in the range (200 - 1000) nm by using UV/V is spectrometer. Photoluminescence was measured (Renishaw 2000) system, and at excitation wavelengths of 300 nm. Electrical properties were measured, concentration and mobility of carrier and Hall effect of film were determined. NiPc/Si heterojunction has been fabricated as in **Figure 1**. Single crystal n-type Silicon wafer was used with phosphor doping, crystal orientation (100), thickness 380 μm and electrical resistivity of 5 - 10 Ω.cm. The wafer from VSM company, USA, Silicon wafer was cleaned using etching process by immersed Si wafer and stirrer them in a solution containing 3 ml HNO_3, 1 ml HF, 2 ml H_2O for (1 - 3) minutes, then immersed in distilled water for several times. Finally, it was dried by blower and

swab in special paper. I-V and C-V(at1kHz) characteristic in the case of darkness and light were achieved for the NiPc/Si Hj cell by digital Keithley, power supply and LRC meter. Solar cell properties and there parameters (β, φ, V_{oc}, I_{sc}, Im, Vm, η etc..) have been achieved at light to the NiPc/Si HJ with optimum thickness and substrate temperature at forward and reverse conditions with intensity 55 mW/cm^2 by using Halogen lamp type Philips of 120 W.

3. Results and Discussion

The FT-IR spectra to NiPc as a material were recorded at RT, a comparison between these spectra of NiPc and H$_2$Pc spectra as in **Figure 2**. It is observed in the range (400 - 2000) cm^{-1} bond bending whereas in the range (2000 - 4000) cm^{-1} the bond stretching. Weak peaks in the range (600 - 400) cm^{-1} which indicate the presence of (metal-Nitrogen) bond vibration at (508 - 578) cm^{-1} which assigned for (Nickel-Nitrogen). The band C-N at (1334 - 1320) 1/cm is, and the peak bond C=C at (1612) cm^{-1} and the peak (1533) cm^{-1} represents Benzene ring band. The spectrum shows the absent of stretching band (N-H) which appears in (H$_2$Pc) spectrum.
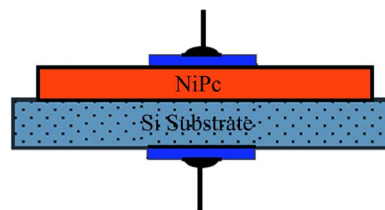
The incident light (I_o) and transmission intensity (I_T) is given by [12] [13]:
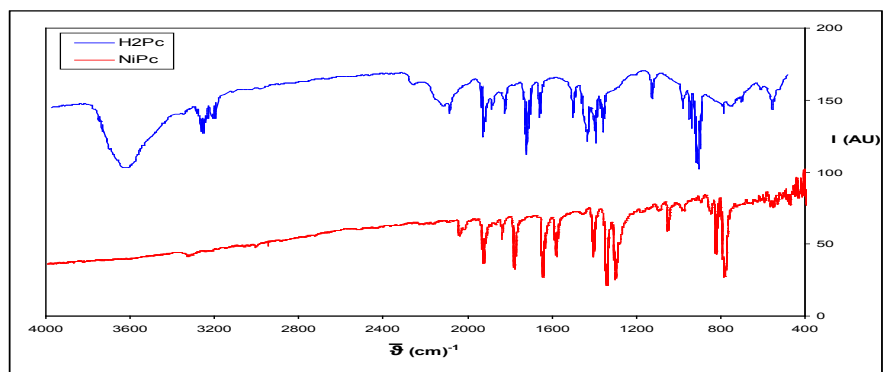
$$I_T = I_o \mathrm{e}^{-\alpha t} \tag{1}$$

The absorption coefficient α and t is thickness of films. The α of film was calculated by absorption and transmission spectra according to:

$$\alpha = \ln T^{-1}/t \tag{2}$$

I_T/I_o is defined as the transmittance (T) [1].


Figure 1. The NiPc/Si heterojunction diagram.

Figure 2. FT-IR spectra for NiPc and for H2Pc powders.

Figure 3 represents the absorbance for Nickel phthalocyanine film at various T_s, it is observed substrate temperature increasing causes absorbance decreases, normally, except in the range (350 - 400) K where there is inverse behavior for Q band and B band, and the variations in (Q) bands less than in B band and minor changes happens in flat area, this behavior because of a good crystal arrangement at high substrate temperatures. It is observed that band of absorption B higher from band of absorption Q. Effect of substrate temperature on absorbance is shown in Figure 4. A red shift in B, Q_1 bands peak positions with substrate temperature increasing has been seen while no change in Q_2 peak position as shown in Table 1.
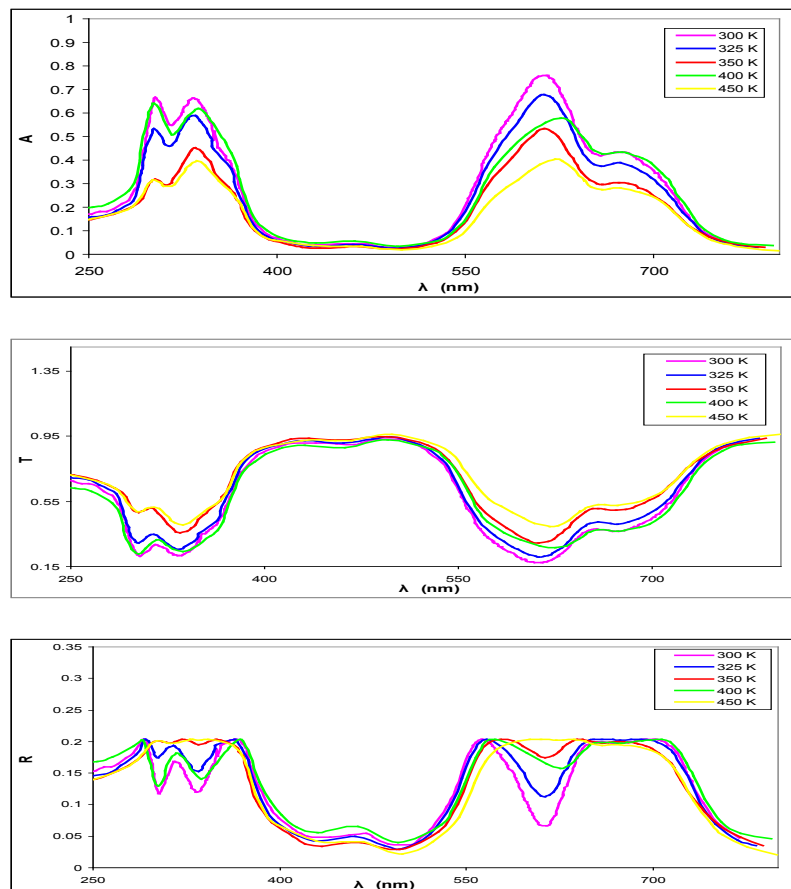
Figure 3. Absorbance, transmittance and reflectance versus λ to Nickel phthalocyanine film at various T_s.
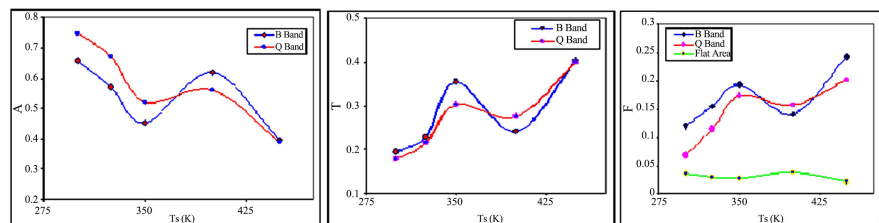
Figure 4. Absorbance, transmittance and reflectance versus T_s for Nickel phthalocyanine film at various Ts. for B and Q bands.

Table 1. Values of maximum absorption peak for NiPc thin films at different substrate temperatures.

Substrate Temperature (K)	B band	Q-band	
	peak position (nm)	Q₁ peak position (nm)	Q₂ peak position (nm)
300	336	616	673
325	336	617	673
350	336	620	673
400	335	625	673
450	342	627	673

Substrate temperature effect on transmittance was studied for NiPc thin films and shows that maximum transmittance was in the range (400 - 500) nm wavelength and clear variations happened in B and Q bands, while the small variations are in flat area. The transmittance spectra for NiPc film at various T_s, are shown in **Figure 3** and **Table 1**.

Effect of substrate temperature on transmittance has been studied, one can see the transmittance increases normally with substrate temperature increase, except in the range of (350 - 400) K where there is a reverse behaviour, and Q band variation in transmittance is smaller than that for B band for same values of T_s as shown in **Figure 3** and **Table 1**.

The reflectance spectra for NiPc film at Ts (300 - 450) K have been done, reflectance was calculated by

$$R = 1 - (A + T) \tag{3}$$

the B and Q bands have high variations in R while the flat area has still minimum variations. At 450 K substrate temperature R takes the same values for wide range and for both bands. The reflectance spectra for NiPc film at various T_s were given in **Figure 3** and **Table 1**.

Substrate temperature variations effect on reflectance of NiPc thin films, where reflectance increases by increase in T_s for B and Q bands except for the range of T_s (350 - 400) K. The reflectance of flat also plotted with T_s it seems to be that it behaves inversely. The effect of T_s on reflectance was given in **Figure 4**. The behaviour in **Figure 4** may be due to recrystalization by increasing temperature and phase transition from β-phase to α-phase [15] [16].

Figure 5 represents the variations in absorption coefficient (α) with wavelengths at various temperatures, the following equation gives α:

$$\alpha = (2.303) A \cdot t^{-1} \tag{4}$$

Absorption represents by (A), and (t) thickness, it is observed the flat area at the range (400 - 500) nm having the same values of absorption coefficient approximately, because this range is the high transmission range; while for B band, absorption coefficient becomes greater than 10^4 cm^{-1} which means high proba-

bility for direct transition. The high absorption coefficient in Q band is due to traps inside energy gap.

Effect of T_s for NiPc film was given in **Figure 6**, absorption coefficient decreases with substrate temperature increases, normally, except in the range (350 - 400) nm a reverse behaviour has been seen that is due to enhancement in crystal structure.

The absorption coefficient (*α*), and types of transition can be deduced from Tauc relation [14]:

$$\alpha h\upsilon = \text{const.}\left(h\upsilon - Eg\right)^{r} \tag{5}$$

where *r* is empirical constant depending on the transition types, where *r* is equal to 1/2 for allowed direct transition, and *hυ* represent photon energy which equals to [13] [14]:

$$h\upsilon(\text{eV}) = 1.24 \cdot \lambda^{-1}(\mu\text{m}) \tag{6}$$

Plank constant was *h*, *υ* is frequency, *λ* represents wavelength. By polting (*αhυ*)² against *hυ* for allowed direct transition, and the absorption coefficient $\alpha \geq 10^4$ m^{-1}, the straight line indicating the transition is allowed direct. Extrapolation of the linear portion of the plot to the *x* axis (*αhυ* = 0) represent the values of energy gap as shown in **Figure 7** [15] [16].
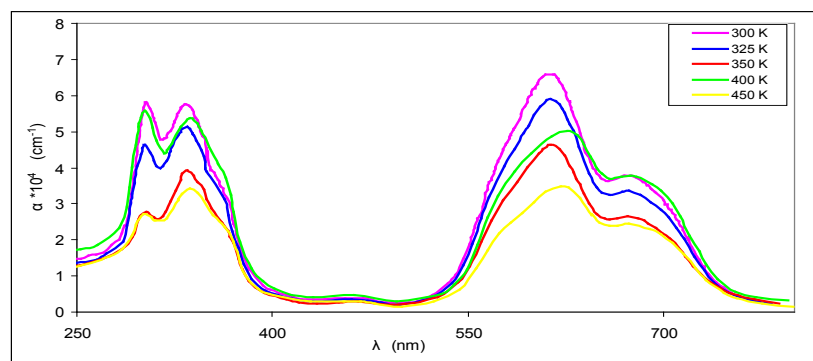
Figure 5. *α* versus *λ* for NiPc films at various T_s.
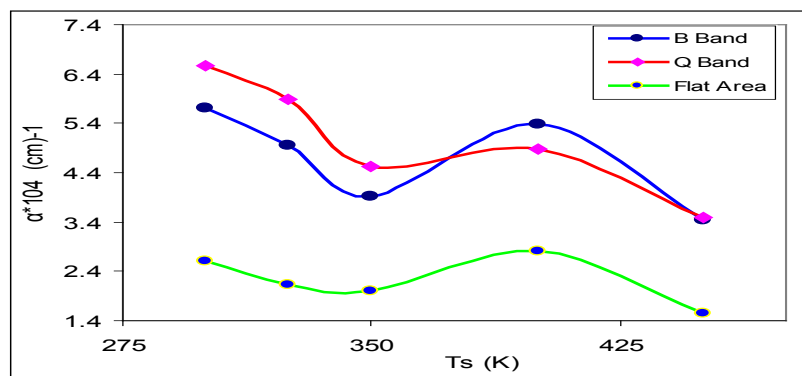
Figure 6. Substrate temperature effect of NiPc thin film on absorption coefficient for B and Q bands.
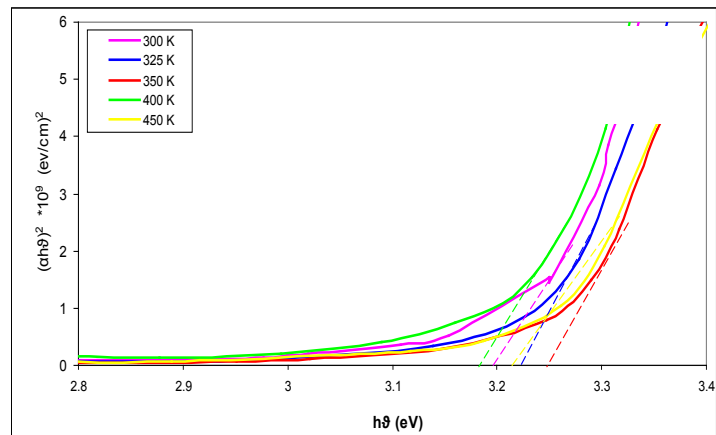
Figure 7. (ahv)^2 vs hv for Nickel phthalocyanine film at various T$_s$.

Values of Eg increases with increasing substrate temperature slightly as given in **Table 2**. This is due to the decrease of defects and improvement in crystal structure of thin prepared films [15] [16].

The optical constants for NiPc thin films at wavelength equal to 500 nm at different substrate temperatures were shown in **Table 3**.

The refractive index (n) can be evaluated from equations [13] [14].

$$n = \left[\left(4R \big/ (R-1)^2 \right) - k^2 \right]^{1/2} - (R+1) \big/ (R-1) \tag{7}$$

where (R) is the reflectance. The extinction coefficient (k) is calculated from [13] [14].

$$k = \alpha\lambda / 4\pi \tag{8}$$

The dielectric constant is:

$$\varepsilon = \varepsilon_1 - i\varepsilon_2 = 1 + 4\pi\varphi \tag{9}$$

(φ) is the sum of polarizabilities resulting from free carries. So that [14]

$$\varepsilon_1 = n^2 - k^2 \tag{10}$$

$$\varepsilon_2 = 2nk \tag{11}$$

Photoluminese spectra have an important role because they give information about the optical properties, likes Eg, excitons, traps and levels of energy. The E$_g$ which calculated from photoluminese spectra (pL) is more precision from Tauc equation. **Figure 8** represents (pL) spectra for Nickel phthalocyanine film at various T$_s$, **Table 4** gives energy gap obtained by PL spectra and by Tauc method at different substrate temperatures with excitation wavelength 315 nm. The lowest value for E$_g$ is at T$_s$ 400 K, it is the same result found by Tauc equation. All E$_g$ values found by PL spectra are greater than that found by Tauc equation method for all studied range of substrate temperatures. Traps in energy gap take part in an important role in organic material conductivity, to study the behavior of traps inside energy gap, two photoluminescence spectra were recorded for NiPc thin films at 110 nm thickness, one using excitation wavelengths 315 nm (where

photons energy greater than E$_g$), and the other about half of energy gap (600 nm). Photoluminescence spectra for two excitation wavelengths are shown in **Figure 9**. It shows the ordinary behavior when NiPc excited by a photon with energy 3.93 eV (excitation wavelength 315 nm) which gives emitting photon with 3.29 eV (wavelength 376 nm). The small peak gives emitting photons with 3 eV which is the Eg approximately. An extra ordinary behavior also happened when NiPc thin film excited by a photon with energy 2.06 eV (wavelength 600 nm) and gives emitting photon with energy 3.6 eV (wavelength 344 nm). The abnormal behavior may refer to nonlinear properties. Photoluminescence spectra for NiPc thin films at thicknesses (110) nm were done using exciting wavelength 600 nm as shown in **Figure 10**. We can see both of two thin films give emitting photon energy about 3.6 eV (wavelength 344 nm). As a result the traps which represented by Q band has great importance in conductivity of NiPc film [15] [16].

Table 2. Substrate temperature effect on Eg and traps for Nickel phthalocyanine film.

| Ts (K)	Eg (eV)	Trap (1) Energy (eV)	Trap (2) Energy (eV)
300	3.21	2.01	1.84
325	3.23	2	1.84
350	3.27	2	1.84
400	3.19	1.98	1.84
450	3.25	1.98	1.84

Table 3. The optical constants for NiPc films with different substrate temperature at λ = 500 nm.

| T_s (K)	$a \times 10^4 (cm)^{-1}$	n	K^*10^{-4}	ε_r	ε_i
300	2.614	1.2295	105	1.511	0.025
325	2.126	1.187	84	1.41	0.02
350	2	1.176	79	1.384	0.018
400	2.806	1.246	11	1.552	0.027
450	1.539	1.136	61	1.291	**0.0139**

Table 4. Energy gap obtained by photoluminescence and Tauc method at different substrate temperatures excitation wavelength 315 nm.

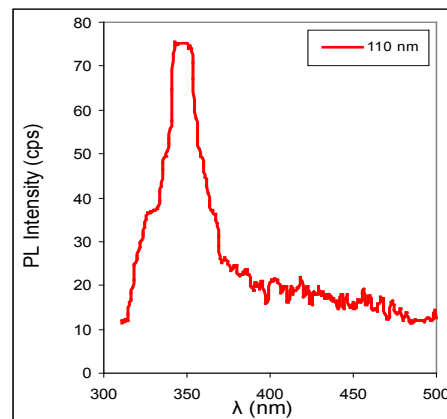| T_s(K)	E_g (PL) (eV)	E_g (Tauc) (eV)	*Error ratio%*
300	3.27	3.21	1.5
325	3.29	3.23	1.8
350	3.29	3.27	0.6
400	3.26	3.19	2.1
450	3.28	3.25	0.9
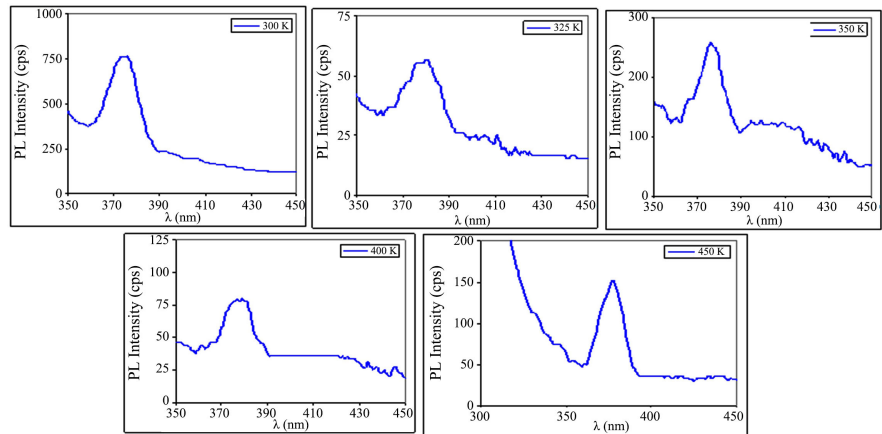
Figure 8. Photoluminescence spectra for Nickel phthalocyanine film at various Ts using excitation wavelength 315 nm.
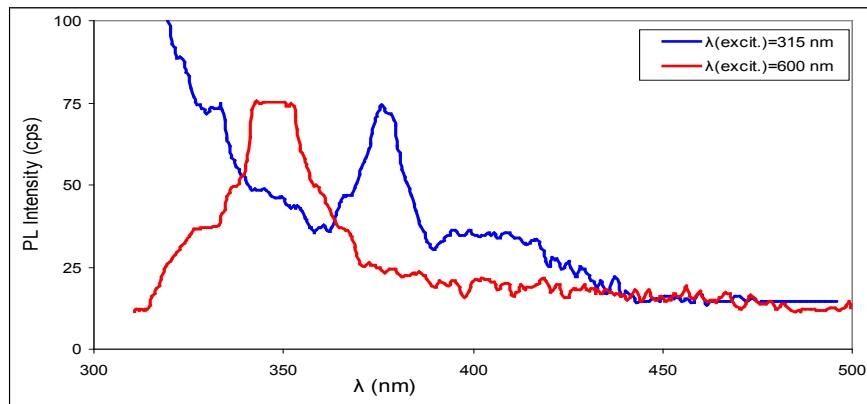
Figure 9. Photoluminescence spectra for NiPc thin films at thickness 110 nm using excitation wavelengths (315 and 600 nm).


Figure 10. Photoluminescence spectra for NiPc thin films at thicknesses (110) nm using excitation wavelength 600 nm.

The D.C. conductivity for NiPc thin films was calculated as listed in **Table 5**, the room temperature conductivity increase as film Ts increases for the (325 - 450) K about five times and this is attributed to better crystallinity (grain size).

By plotting $\text{Ln}\sigma$ versus of $10^3/T$ as shown in **Figure 11**, activation energy (E_a) can be determined. The electronic transport mechanism is influenced by the inter-grain boundaries. As it is observed from **Figure 11**, there are three activation energies within the range (298 - 473) K as in **Figure 11** and **Table 5** and this conformed by [17] [18].

As shown in **Figure 12**, the activation energy (E_a) values vary with T_s due to variations crystalline structure of the prepared film [17].
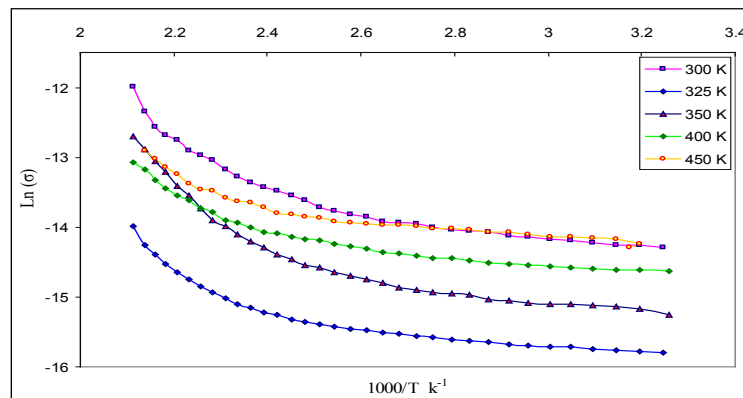
**Figure 11.** $\text{Ln}\sigma$ versus of $10^3/T$ to film of NiPc for various Ts.
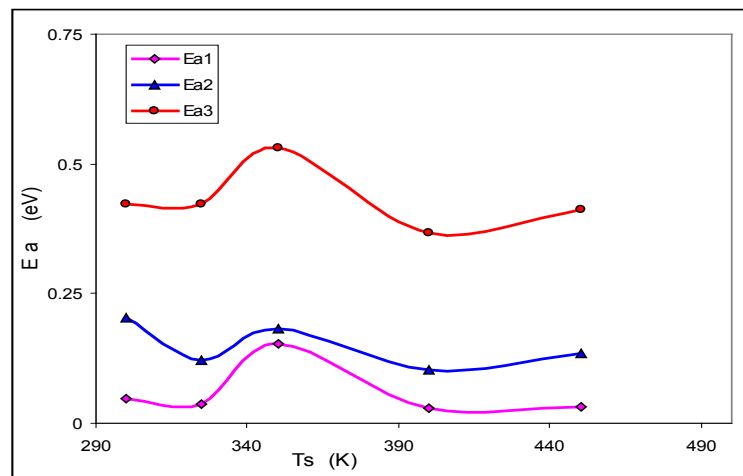
Figure 12. Effect of T_s on E_a for Nickel-Pc films.

**Table 5.** The electrical parameters: Ea, and $\sigma_{R.T}$ for Nickil phthalocyanine film for various Ts.

| Ts(K)	$\sigma_{R.T} \times 10^{-7}$ $(\Omega.cm)^{-1}$	E_{a1} (eV)	Temp. Range (K)	E_{a2} (eV)	Temp. Range (K)	E_{a3} (eV)	Temp. Range (K)
300	6.22	0.0478	308 - 378	0.2044	393 - 433	0.4223	433 - 468
325	1.377	0.037	308 - 336	0.121	388 - 428	0.423	438 - 468
350	2.382	0.182	307 - 368	0.182	372 - 423	0.53	428 - 473
400	4.459	0.03	307 - 358	0.104	373 - 423	0.368	433 - 473
450	6.807	0.033	307 - 393	0.135	393 - 443	0.411	443 - 473

Carrier concentration (n) can be calculated which decreases from (10 - 0.302) cm^{-3} for Ts (325 - 450) K except at 300 K, and P-types films have been observed by Hall effects, whereas the carriers mobility (μ) up from 0.03 (cm^2/v.s.) to 99.42 (cm^2/v.s.) by increasing T_s from (325 - 450) K for prepared films except at 300 K, and this is given in Table 6. From the Table the carrier mobility increases with substrate temperature except at 300 K while the carrier concentration decreases with increases of substrate temperature [17] [18].

p-NiPc/n-Si solar cells have been fabricated thermally by deposited the organic material NiPc on n-type silicon wafer, at substrate temperatures of (300, 400) K with 265 nm thickness. The characteristic of Capacitance (C)-Voltage (V) have been described at RT for P-NiPc/n-Si HJ at substrate temperatures of (300, 400) K. It is observed from Figure 13. By increasing of bias voltage the values of C are decreases, due to the higher values of depletion width (W) leading to increase of built-in voltage (V_{bi}). By plotting C^{-2} with reverse voltage bias (Figure 14) the intersection $C^{-2} = 0$ represent V_{bi}. It is observed from this figure increase in built-in potential with high temperatures, Reason for this is improvement in structural defects and the progress films during deposition (*i.e.* grain boundaries, stacking faults), as shown in Table 7.
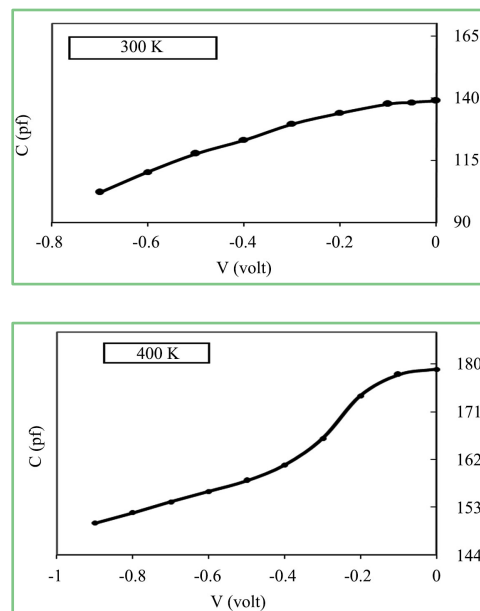
Figure 13. The capacitance of NiPc/Si HJ versus reverse bias voltage, for Ts (300, 400) K.
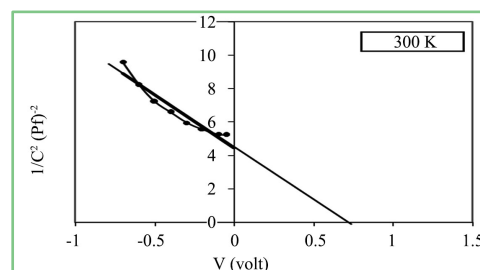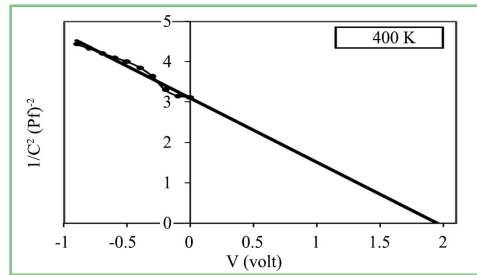
Figure 14. The variation of the inverse capacitance squared for NiPc/Si HJ with the reverse bias voltage for Ts (300, 400) K.

Table 6. n and μ for NiPc film at various Ts.

$T_s(K)$	$n*10^{12}(cm^{-3})$	$\mu(cm^2/v. s.)$
300	0.396	72.74
325	10.8	0.030
350	2.75	8.922
400	0.480	73.4
450	0.302	99.42

Table 7. The capacitance at zero bias voltage C_o, and built-in potential V_{bi} for the p-NiPc/n-Si.

Thickness (*nm*)	Ts (K)	C_o (*pf*)	V_{bi} (Volt)
265	300	140	0.69
265	400	180	1.7

Figure 15 represents the current-voltage characterization for NiPc-Silicon HJ for both biases in the dark at substrate temperatures of (300, 400) K. These curves showed the conduct of the current at two bias of voltage. From **Figure 15**, two regions have been observed at forward current. From (0 - 0.2 V) for recombination current, and from 0.2 V to 0.4 V represents the tunneling current. Also the current at reverse bias voltage contains two regions for generation and diffusion process.

Figure 16 gives the semi logarithmic plot of the current-voltage Curve, the initial part voltage range (0 - 0.2) Volt could be approximated by an expression of the type I~exp(qV/βk$_B$T). So the ideality factor β has been calculated and it is about 0.613 - 0.734 which indicate on the mechanism of conduction is generation and diffusion.

The series resistance (**R$_s$**) and shunt resistance (**R$_{sh}$**) of the junction can be evaluated by plotting resistance of junction (R$_j$) versus applied voltage as in **Figure 17** and **Table 8** gives these parameters of two NiPc/Si HJ samples.

The main factor for working of solar cell is photocurrent (Iph). The photocurrent for NiPc/Si HJ at substrate temperatures of (300, 400) K were plotted against reveres and forward bias as shown in **Figure 18**, V_{oc}, I_{sc} were determined

by the intersect of photocurrent curve with x and y axis. Also maximum voltage (V_m) and current (I_m) for solar cell were found, full factor (F.F) and efficiency (η) have been calculated. For HJ under illumination, the photocurrent increases with increasing of voltage which leads to separate electrons and holes and then increases the photocurrent to higher values. The light current depends on the processes of generation and diffusion. The results comparison tabulated in Table 9 leads to that the selected thickness and substrate temperatures are a good choice, where the results of photocurrent parameters increase with increasing substrata temperatures.

**Table 8.** The values of β, Is, φ_b, R_{sh} and R_s for substrate temperatures of (300, 400) K.

T(K)	β	$I_s(\mu A)$	$\varphi_b(V)$	$R_{sh}(K\Omega)$	$R_s(K\Omega)$
300	0.61	0.54	2.53	3.76	0.24
400	0.734	0.23	3.69	2.58	0.23

Table 9. The values of V_{oc}, I_{sc}, V_m, I_m, J, P_{Max}, F.F and η for substrate temperatures of (300, 400) K.

| Sample no.	V_{oc} (v)	I_{sc} (mA)	V_m (v)	I_m (mA)	J (mA.cm^{-2})	P_{Max} (miliwatt)	F.F	η %
1	0.335	2.77	0.24	1.77	11.08	0.4248	0.457	3.08
2	0.415	4.26	0.25	2.77	17.04	0.6925	0.391	5.03
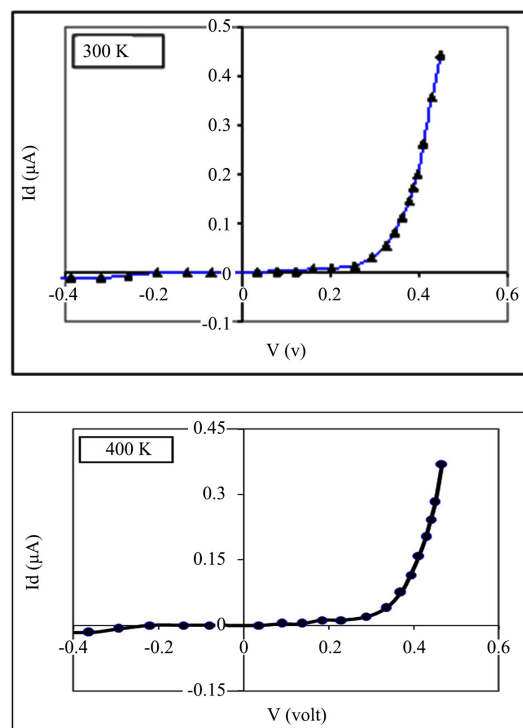
Figure 15. I-V characteristics for NiPc-Silicon HJ for T_s (300, 400) K in case of darkness at forward bias and reverse bias.
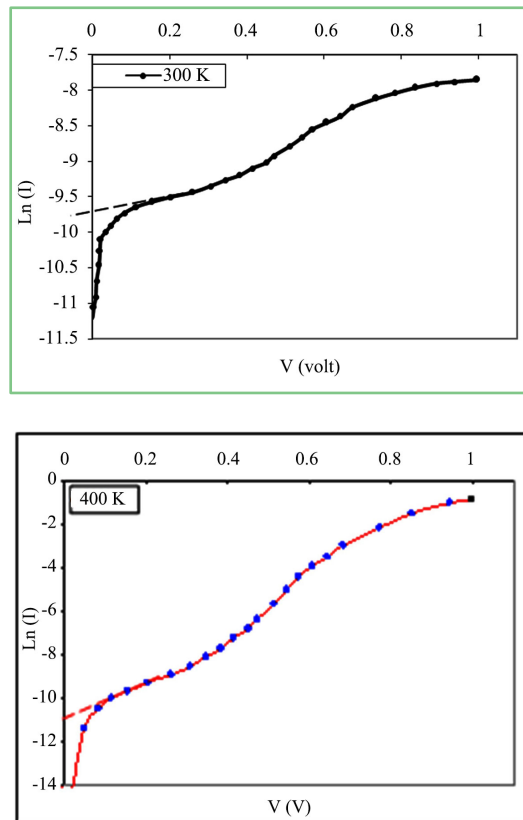
Figure 16. Semi logarithmic plot of the I-V characteristics for NiPc-Silicon HJ at forward bias voltage for T_s (300, 400) K in case of darkness.
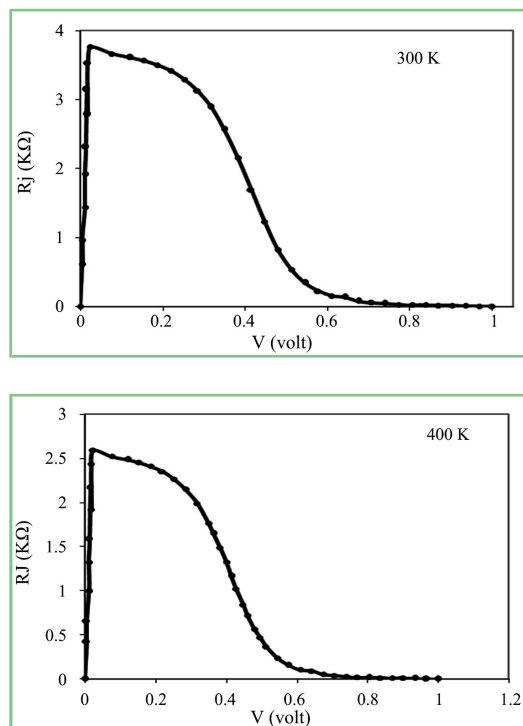
Figure 17. The junction resistance with the external applied voltage for substrate temperatures of (300, 400) K.
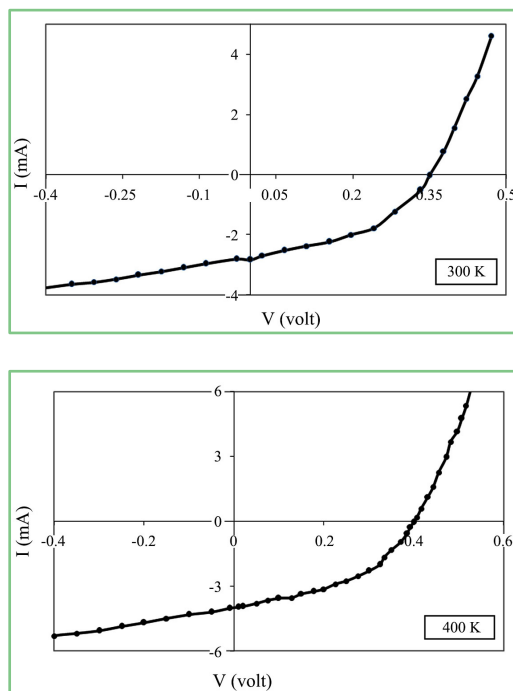
Figure 18. The photocurrent for NiPc/Si HJ for substrate temperatures of (300, 400) K.

4. Conclusions

Thermally evaporated Ni-Pc film with various substrate temperatures was prepared excellently. It was found that all E_g values found by PL spectra are greater than those found by Tauc equation method for all studied range of substrate temperatures. Fluorescence spectra confirmed the splitting of soret band. The energy gap values are increased by raising the base temperature. There are three activation energies increasing with the increase of substrate temperatures. P-types films have been observed by Hall effects. Carrier concentration and mobility have been reduced by increasing of substrate temperatures. Results of photocurrent parameters increase with increasing substrate temperatures. The maximum efficiency was obtained around 5% at thickness of 265 nm and 400 K. The results indicate that the selected thickness and substrate temperatures are a good choice for solar cell applications.

Conflicts of Interest

The authors declare no conflicts of interest regarding the publication of this paper.

References

[1] El-Nahass, M.M., Bahabri, F.S. and Al-Harbi, S.R. (2001) Optical Properties of Copper Phthalocyanine (CuPc) Thin Films. *Egyptian Journal of Solids*, **24**, 307-311.

[2] Yanagi, H., Kouzeki, T. and Ashda, M. (1992) Molecular Orientation of Vacuum-Deposited Thin Films of Zinc Naphthalocyanine. *Journal of Applied Physics*,

71, 5146-5153. https://doi.org/10.1063/1.350569

[3] Burgess, A.N. (1987) Comparison of Transient Thermal Conduction in Tellurium and Organic Dye Based Digital Optical Storage Media. *Journal of Applied Physics*, **61**, 74. https://doi.org/10.2307/40142489

[4] Dini, D., Barthel, M. and Hanack, M. (2001) Phthalocyanines as Active Materials for Optical Limiting. *European Journal of Organic Chemistry*, **9**, 3759-3769. https://doi.org/10.1002/1099-0690(200110)2001:20<3759::AID-EJOC3759>3.0.CO;2-U

[5] Liu, Z.T., Kwok, H.S. and Djurisic, A.B. (2004) The Optical Functions of Metal Phthalocyanines. *Journal of Physics D: Applied Physics*, **37**, 678. https://doi.org/10.1088/0022-3727/37/5/006

[6] Kumar, G.A., Jose, G., Thomas, V., Unnikrishnan, N.V. and Nampoori, V.P.N. (2003) NIR to UV Absorption Spectra and the Optical Constants of Phthalocyanines in Glassy Medium. *Spectrochimica Acta Part*, **59**, 1-11. https://doi.org/10.1016/S1386-1425(02)00037-9

[7] Raji, P., Sanjeeviraja, C. and Ramachandran, K. (2005) Thermal and Structural Properties of Spray Pyrolysed CdS Thin Film. *Bulletin of Materials Science*, **28**, 233-238. https://doi.org/10.1007/BF02711253

[8] Hendi, A.A. (2011) Determination and Analysis the Influence of X-Ray Irradiation on Optical Constant of Magnesium Phthalocyanin. *Australian Journal of Basic and Applied Sciences*, **5**, 38-44.

[9] Hussein, M.T., Nasir, E.M. and Al-Aarajiy, A.H. (2013) Structural and Surface Morphology Analysis of Nickel Phthalocyanine Thin Films. *Advances in Materials Physics and Chemistry*, **3**, 113-119. https://doi.org/10.4236/ampc.2013.31A014

[10] Joseph, B. and Menon, C.S. (2007) Studies on the Optical Properties and Surface Morphology of Nickel Phthalocyanine Thin Films. *E-Journal of Chemistry*, **4**, 255-264. https://doi.org/10.1155/2007/643834

[11] Pustelny, T., Ignac, J., Jarzabek, B. and Burian, A. (2004) Optical Investigation Concerning Layered Metal Phthalocyanine Nanostructures Affected by NO_2. *Optica Applicata*, **34**, 551-561.

[12] Hummel, R.E. (2001) Electronic Properties of Materials. 3rd Edition, Springer, New York.

[13] Schroder, D. (1990) Semiconductor Material and Device Characterization. John Wiley & Sons, Hoboken.

[14] Pankove, J.L. (1971) Optical Processes in Semiconductors. Prentice-Hall, Englewood Cliffs.

[15] Hussein, M.T., Nasir, E.M. and Al-Aarajiy, A.H. (2012) Study on the UV-Visible of Ni-Phthalocyanine Thin Film Optical Properties. *International Journal of Thin Films Science and Technology*, **1**, 71-76.

[16] Hussein, M.T., Eman, M.N. and Senaed, F.A. (2014) Optical Properties of Cobalt Phthalocyanine Thin Films. *Indian Journal of Research*, **3**, 145-147.

[17] Hussein, M.T., Eman, M.N., Thekra, K. and Senaed, F.A. (2014) Study the Effect of Annealing Temperature on the Structural, Morphology and Electrical Properties CoPc Thin Films. *International Journal of Current Engineering and Technology*, **4**, 3263-3269.

[18] Nasir, E.M., Hussein, M.T. and Al-Aarajiy, A.H. (2019) Impact Thickness on Structural and Electrical Characterization of Nickel Phthalocyanine Thin Films. *Advances in Materials Physics and Chemistry*, **9**, 123-132. https://doi.org/10.4236/ampc.2019.97010